

# Venusian Impact Crater Analysis

Matthew Petersen

May 18, 2016

## 1 Background

The impact craters of Venus are pristine and well-preserved, albeit small in number. 937 Venusian craters are recorded in the crater database of Herrick et al.[3], some of which exhibit wedges of avoidance. The wedge of avoidance is a characteristic feature of oblique impacts, and are found on several bodies in the Solar System, including Mars, the Moon, and others, as well as Venus. The feature is characterized by a gap in the ejecta deposits uprange of the crater. The cutoff angles for these features have been investigated by Herrick and Forsberg-Taylor[4], and are based on the cumulative population numbers given by  $n = \sin(i)^2$ , where  $n$  is the total fraction of the population with an impact angle below  $i$ [1]. For Venus, the cutoff angle associated with a section of rim without ejecta is given as  $30^\circ$ , with a cumulative fraction of craters of around 0.4[4, p. 1563]. This fraction is taken by Herrick and Forsberg-Taylor from the population of craters with a diameter greater than 30 km. The smaller sample was chosen to take into account the strong

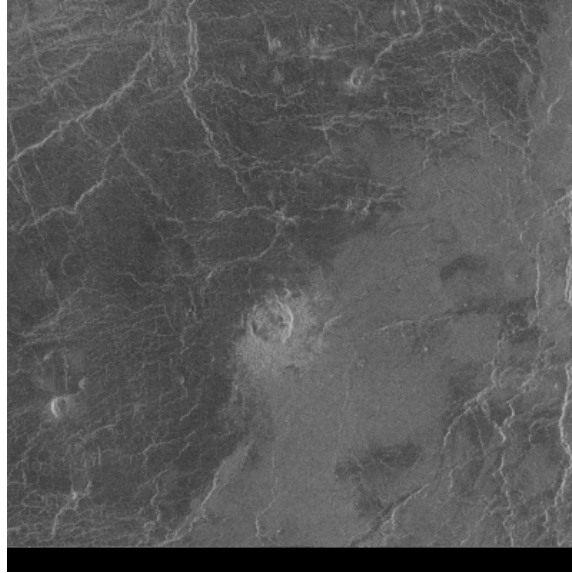
atmospheric screening that occurs on Venus. The dense layers of the Venusian atmosphere play a strong part in filtering out smaller impactors, and this could cause deviation from the  $n = \sin(i)^2$  law at small impactor sizes.

While a set of cutoff angles has been calculated for various degrees of asymmetry in craters[4], no scaling law exists to relate the angle of impact to the breadth of the wedge of avoidance.

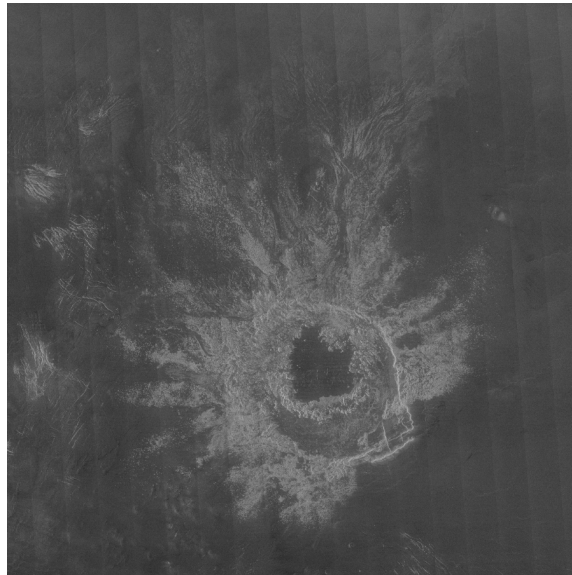
## 2 Methodology

A MATLAB script was written that would scrape crater data from the crater database available online, along with images for each of the craters (when available). A pre-screening round was performed, whereby the whole corpus of craters was visually inspected to determine whether a clear wedge of avoidance was present, and whether the image was clear enough to distinguish a wedge; this created a smaller set of craters on which the more in-depth visual analysis was performed. An example of this distinction can be seen in figure 1. Many images were not suitable to analysis, for many reasons; some did not have visible wedges present, some had radar image artifacts, and some were too poorly preserved to analyze. In total, 51 images were chosen for further analysis, representing 5.4 percent of the total crater population.

In order to measure the azimuthal breadth of the wedge of avoidance, a simple method was developed to be easily implemented across the entire sample size. A set of five points was chosen on each image, as seen in figure 2. The point P0



(a) Crater Ayashe, rejected from further inspection



(b) Crater Marie Celeste, accepted for further analysis

Figure 1: Example choices made for image acceptance or rejection

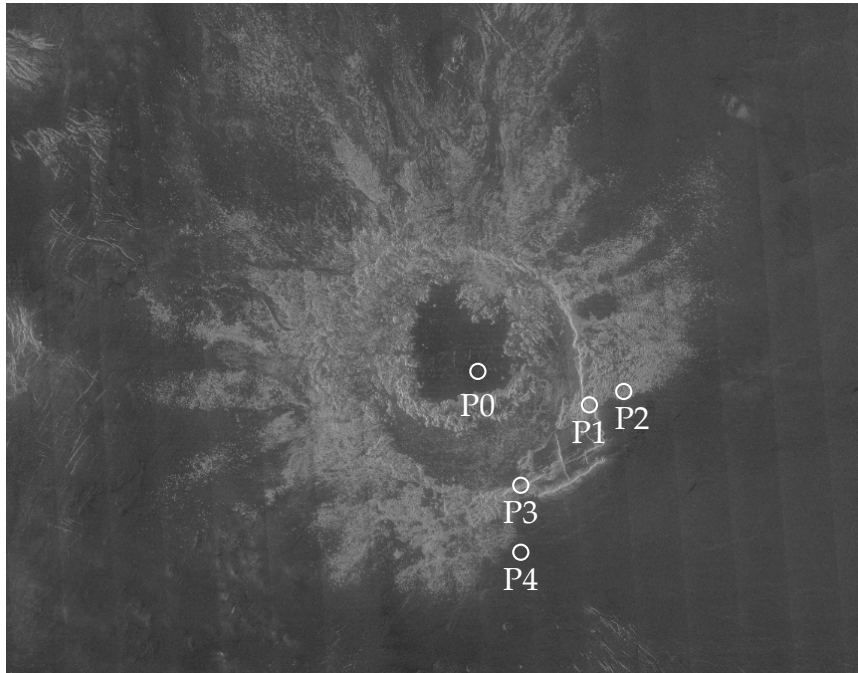


Figure 2: Order of point selection

marks the approximate center of the crater. P1 and P3 mark the counterclockwise and clockwise points where the wedge intersects the rim. P2 and P4 mark points on the edges of the wedge of avoidance that are further out from the rim. These points were chosen using a small set of criteria. The point had to be located on a part of the edge that was clearly distinguishable from the surrounding terrain. In addition, a consideration had to be made of the sometimes-curving edges of the wedge of avoidance. The edges were visually inspected to find a location for the point that was farther out on the edge while still being on the straighter section of the wedge edge. The selection of points was used to define two lines, the angle between which was taken as a measure of the breadth of the wedge of avoidance.

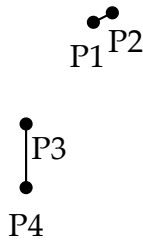


Figure 3: Lines used for angle measure

### 3 Results and Discussion

#### 3.1 Data

The data, presented in histogram form in figure 4, shows a distribution of impact angles with a peak near  $120^\circ$ . The average breadth is  $105.3^\circ$ , with a standard deviation of  $28.5^\circ$ . A cumulative plot from  $30^\circ$  to  $180^\circ$  is shown in figure 5. The cumulative count was used to calculate an estimated impact angle using the  $n = \sin(i)^2$  relation, which is shown in figure 6. This gives an impact angle cutoff near  $12^\circ$ . This is a very low impact angle, and is not in agreement with the results derived by Herrick and Forsberg-Taylor. Filtering craters with a diameter below 30km, the cumulative count in figure 7 and the impact angle plot in figure 8 were calculated. These give an impact angle cutoff near  $25^\circ$ , which is much closer to the angle given by Herrick and Forsberg-Taylor.

#### 3.2 Effect of Diameter

The effect of crater diameter on wedge breadth is unclear; Shuvalov finds a general dependence on impact scale for crater asymmetry[5], while Herrick and Hessen

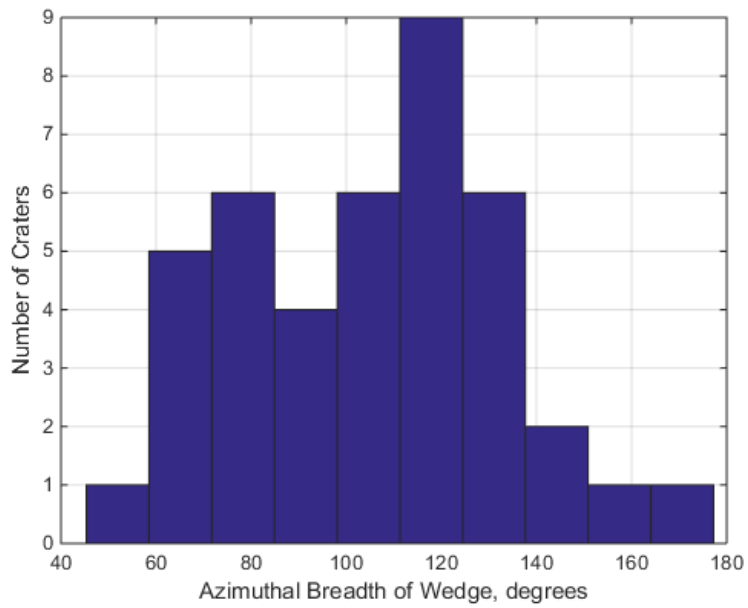


Figure 4: Data from visual inspection

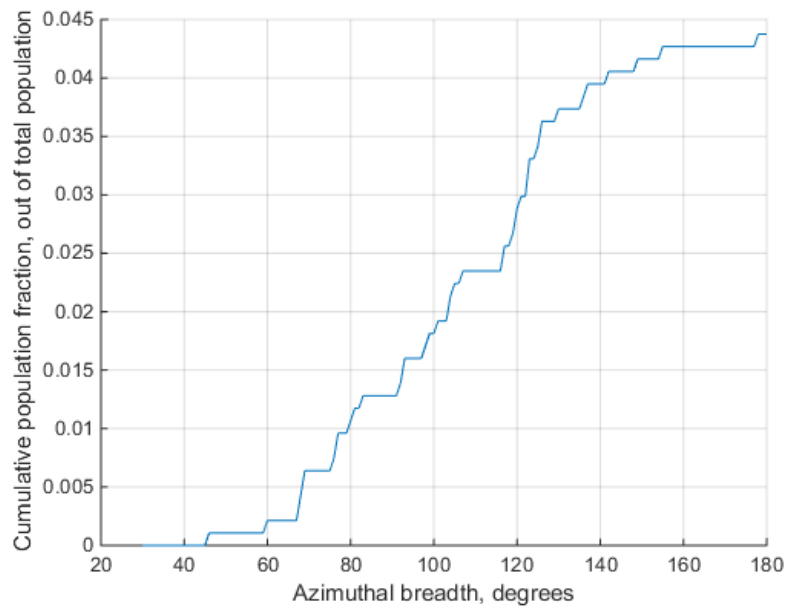


Figure 5: Cumulative plot with total population

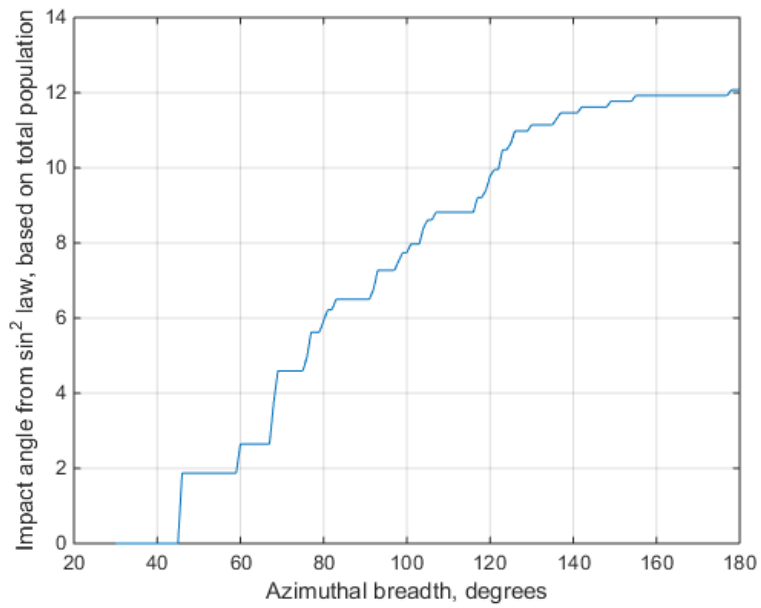


Figure 6: Impact angle relation for total population

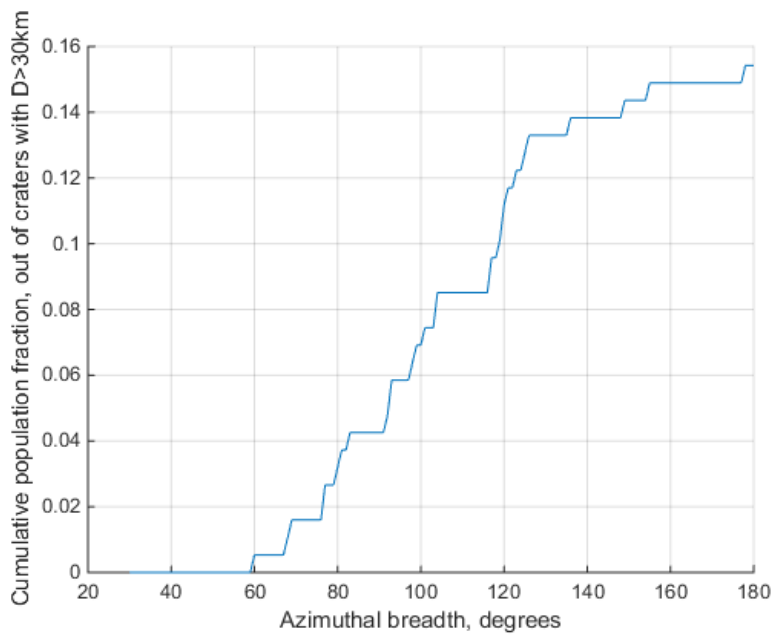


Figure 7: Cumulative plot with  $D > 30\text{km}$  population fraction

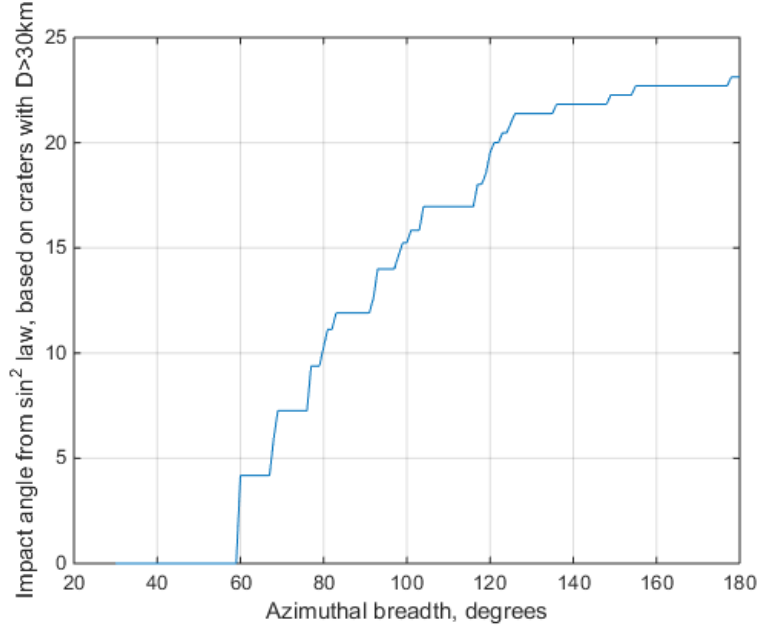


Figure 8: Impact angle relation for  $D > 30\text{km}$  population fraction

does not include a consideration of the effect of diameter. Included in figure 9 is a scatter plot of impact angle versus diameter. There is not an enormous amount of correlation seen in the data, with  $R = 0.083$ . However, a gap in the data does appear; the craters are not distributed uniformly across the range of the parameters. Above a crater diameter of roughly 60km, no craters are present with an azimuthal breadth below 100°. The significance of this gap is unclear; however, it is possible that a phenomenon similar to that described by Shuvalov is in action: the ejecta blanket around larger craters or craters in larger gravity should be larger than that around smaller craters or craters in smaller gravity at the same impact angle[5, p. 1]. This biasing effect could lead to a seeming dearth of high-symmetry craters at larger sizes.

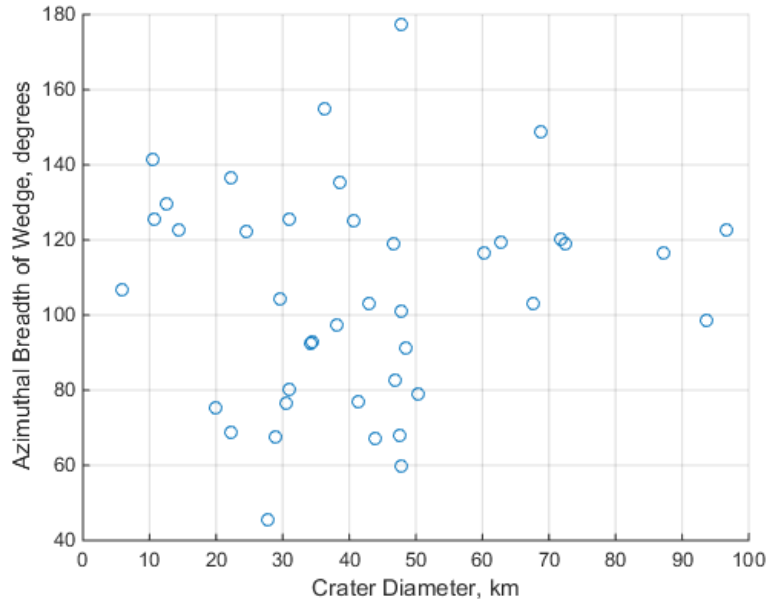


Figure 9: Scatter plot of impact angle and diameter

### 3.3 Scaling Relation

The scaling relation between impact angle and azimuthal breadth was fitted to a sine curve, equal to

$$Az = 68.6\left(\arcsin\left(\frac{\phi}{22.96}\right) + 0.7471\right) \quad (1)$$

In the inverse case, the function is

$$\phi = 22.96 \sin(0.01458Az - 0.7471) \quad (2)$$

Both forms take and return angle values in degrees. This relation is shown plotted in figure 10 with the impact angle plot seen in figure 8. For this fit, an  $R^2$  value of

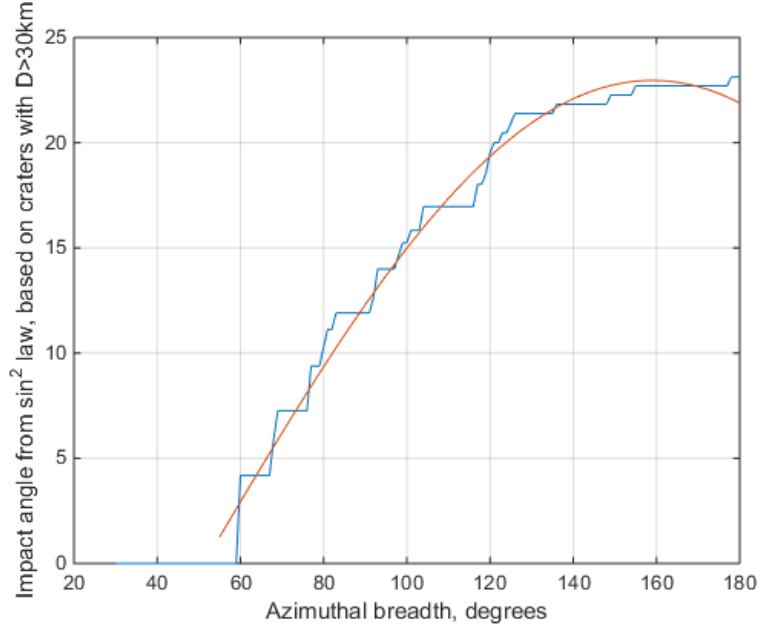


Figure 10: Fit curve plotted with impact angle distribution for craters  $D > 30\text{km}$

0.9897 was found. This fit is only reliable for impact angles below  $25^\circ$ , which was the highest value of impact angle derived from the data. However, it is a good fit for azimuthal breadths between  $\approx 60^\circ$  and  $\approx 160^\circ$ .

This relation is obviously not necessarily robust, and the sample size is possibly too small to justify using it as a measurement tool. In the future, more work could be done to better characterize craters. A larger number of human operators measuring the angles of each crater multiple times would likely be able to provide better-quality azimuthal breadth data. Better training and knowledge of how to identify wedges of avoidance in the radar images would also increase data quality. In addition, a further accounting of the effect of atmospheric screening on the impact angle-population distribution would be helpful to determine what choice of

populations (large diameter vs. all craters) will give the best sense of the relation between impact angle and the size of the wedge of avoidance.

## References

- [1] G. Karl Gilbert. *The moon's face: a study of the origin of its features*. Washington: Philosophical Society of Washington, 1893.
- [2] R. R. Herrick and K. K. Hesses. "The planforms of low-angle impact craters in the northern hemisphere of Mars". In: *Meteoritics & Planetary Science* 41 (2006), pp. 1483–1495. doi: 10.1111/j.1945-5100.2006.tb00431.x.
- [3] R. R. Herrick et al. "Morphology and Morphometry of Impact Craters". In: ed. by S. W. Bougher, D. M. Hunten, and R. J. Phillips. U. of Arizona Press, 1997, pp. 1015–1046.
- [4] Robert R. Herrick and Nancy K. Forsberg-Taylor. "The shape and appearance of craters formed by oblique impact on the Moon and Venus". In: *Meteoritics & Planetary Science* 38.11 (2003), pp. 1551–1578.
- [5] Valery Shuvalov. "Ejecta deposition after oblique impacts: An influence of impact scale". In: *Meteoritics & Planetary Science* 46.11 (2011), pp. 1713–1718.